ORIGINAL ARTICLE

A C G publications

Org. Commun. 14:4 (2021) XX-XX

organic communications

The computational screening of inhibitor for black fungus and white fungus by D-glucofuranose derivatives using in silico and SAR study

Ajoy Kumer [1,2*], Unesco Chakma [3], Mohammed M. Matin [4], Shopnil Akash [5], Akhel Chandro [6] and Debashis Howlader [3]

[1]*Department of Chemistry, European University of Bangladesh, Gabtoli, Dhaka-1216, Bangladesh*
[2]*Department of Chemistry, Bangladesh University of Engineering and Technology, Dhaka-1000, Bangladesh*
[3]*Department of Electrical and Electronics Engineering, European University of Bangladesh, Gabtoli, Dhaka-1216, Bangladesh*
[4]*Bioorganic and Medicinal Chemistry Laboratory, Department of Chemistry, University of Chittagong, Chittagong, 4331, Bangladesh*
[5]*Department of pharmacy, Daffodil International University, Sukrabad, Dhaka-1207, Bangladesh*
[6]*Faculty of Animal Science & Veterinary Medicine, Department of Poultry Science, Sher-e-Bangla Agricultural University, Dhaka, Bangladesh*

(Received August 28, 2021; Revised December 10, 2021; Accepted December 17, 2021)

Abstract: Black fungus is the foremost life-threatening disease during the SARS-CoV-2 affected patients and spreading quickly in the region of the subcontinent of India although there was no prescribed proper medication. As the D-glucofuranose and its derivatives are reported to show strong antifungal activity, this study has been designed with them for their computational investigation. Firstly, the overall prediction of activity spectra for substances (PASS) value illustrates a good probability to be active(Pa) and probability to be inactive (Pi) value. Next, pharmacokinetics parameters including drug-likeness and Lipinski's rules, absorption, distribution, metabolism, excretion, and toxicity (ADMET) parameters, and overall quantum calculation of computational approaches by Density Functional Theory (DFT) have gradually been performed to analyze quantum calculations. After the analysis of docking score, it is found at -9.4 kcal/mol, -7.5 kcal/mol, -7.8 kcal/mol, -8.5 kcal/mol against the strain of black fungus protein strains Mycolicibacterium smegmatis, Mucor lusitanicus, Rhizomucor mieh, and white fungus protein Candida Auris, Aspergillus luchuensis and Candida albicans. Next, the molecular dynamics of docked complexes have been performed to check their stability in biological systems with water ranging 100 ns calculating the Root Mean Square Deviation (RMSD) and Root Mean Square Fluctuation (RMSF) where the minimum RMSD and RMSF value indicated the higher stable configuration of docked complexes. These compounds have perfectly matched all the pharmacokinetics criteria to be a good drug candidate against both black and white fungus, and they are non-carcinogenic, low solubility, low toxic for both aquatic and non-aquatic. In addition, the quantum calculation using DFT conveys the strongest support and information about their chemical stability and biological significance. Finally, it could be concluded that the carboxylic group and methyl group in the benzene ring causes higher binding affinity against black and white fungus protein strain through the formation of hydrogen and hydrophobic bonds.

Keywords: DFT; PASS predication; docking; molecular dynamics; ADMET.

* Corresponding author: E-Mail: kumarajoy.cu@gmail.com

The article was published by ACG Publications
http://www.acgpubs.org/journal/organic-communications © October-December 2021EISSN:1307-6175
DOI:http://doi.org/10.25135/acg.oc.116.2108.2188
Available online: December 24, 2021

1. Introduction

In the last two decades,there have been complaints that the patients with fungal infection have been considered as the life-threatening problems,[1] such as crucial phase in surgical place,[2]zygomycotic,[3]Alzheimer'sdisease,[4] epidemiologic surveillance,[5] lung,[6]epidemiology,[7] immunocompromised patients,[8] acute leukemia,[9] lung transplantation,[10] liver transplantation,[11] hospital renovation,[12] mucormycosis.[13,14]It is estimated that fungal infections caused 25.0–73.7 percent of all SARS-related deaths.[15-17]People with COVID-19, who have had trauma or uncontrolled diabetes mellitus, are more susceptible to cause mucormycosis infection[18-20,] which is commonly known as black fungus [21]and frequently affects the sinuses lungs, skin, and the brain [22,23]. A study reported that mucormycosis (black fungus) was the third most aggressive fungal infection observed in haematological and organ transplantation patients [19,24,] and the most fungal strains such as *Mycolicibacterium smegmatis*, *Mucor lusitanicus*, *Rhizomucor mieh* are responsible for the black fungal infection.[25,26] Another concern occurred during the COVID-19 pandemic due to white fungus infection caused by *Candida* and *Aspergillus* species of fungi.[27] White fungus are often more life-threatening pathogens for COVID-19 patients compared to black fungus infections due to its immediate effects on the lungs and other body organs and spreads and damages key organs, like kidney, brain, private parts, and mouth.[28-31] *Candida auris*, *Aspergillus luchuensis*, and *Candida albicans*are considered to cause the white fungal infection.[32]

A common group of antifungal drugs isazoles, and theyare globally used against both black and white fungus. But studies have found that azole is already-resistant against black and white fungus strains in India.[33] Researchers have also found that white fungus (Candida) is also resistant to multiple drugs.[34]Several pre-existing antifungal medications (Amphotericin B) are used to treat black and white fungus diseases. However, it is a matter of sorrow that this Amphotericin B is also found resistant against *Aspergillus fumigatus*.[35] Still, it is not possible to find an effective medication against white and black fungus.[36,37] It is estimated that the D-glucofuranose and its derivatives had to convey a study on antifungal potential,[38] antibacterial and antiviral activities.[39-42] Regarding this fact, this study has been designed against black and white fungus protein strains through computational tools such as molecular optimization by DFT, molecular docking, PASS prediction, molecular docking, and ADMET properties.

Since this deadly black and white fungus disease are spreading very fast, there is no effective drug.[43] Therefore, effective medicine is critical to prevent these diseases. So, to design an effective drug against black fungus and white fungus, the computational method is followed, the most persuasive approach with low cost and less time consumption. This new technology (Computational Chemistry) creates a new era to build effective medication and design the new biological substance in a short period that reduces costs and time.[44-48]

2. Experimental

2.1. PASS Predication

The PASS prediction data has been collected (Pa>Pi value) from the PASS online website "http://way2drug.com/PassOnline/predict.php". After opening the PASS online software, the Pa>Pi value was collected from selected molecules with their SMILES which showed all the values in a Table. This value of PASS predication means it investigates and evaluates the biological potential of a drug candidate molecule.[49]

2.2. Optimization and Ligand Preparation

Molecular optimization was performed with the help of a technique called DFT functional by utilizing vibrational frequency from the DMol3 code of Material Studio 08.[50.51] The functional, B3LYP, and basis set, DNP+,were utilized for the setup of functions in DMol3 code to obtain extremely precise results, as an electronegative atom, oxygen, seemed to be present. The analytical techniques were utilized after optimizing to build the frontier molecular orbitals (HOMO and LUMO), and the magnitude of HOMO, LUMO. The optimized chemical molecules were exported as a pdb file for future computational work including molecular docking, molecular dynamics, and ADMET.

2.3. Preparation of the Protein

The black fungus strains, such as *Mycolicibacterium smegmatis* (7D6X, Resolution: 2.88 Å),[52]*Mucor lusitanicus* (6ZDW, Resolution: 1.65 Å),[53]*Rhizomucor mieh* (4WTP, Resolution: 1.30 Å),[54]and white fungus strains -*Candida auris* (6U8J, Resolution: 2.49 Å),[55] *Aspergillus luchuensis* (1BK1, Resolution:2.00 Å)[56]and

Candida albicans(5HW7, Resolution: 2.29 Å)[57]- crystal structure was downloaded from the Protein Data bank (PDB) of RCSB Protein web portal. Using PyMOL software version V2.3 (https://pymol.org/2/) [58], protein purification was completed carefully elimination of ligand and water. Once the excess water and Ligand are cleaned, the crystal structure of the cleaned protein file is loaded into AutoDock Tools and followed the instruction to obtain the pdbqt file format.

2.4. Molecular Docking

Molecular docking mainly investigated the binding affinity of biologically active compounds against pathogenic protein stains. The docking procedure was performed with the help of AutoDock Vina incorporated with PyRx Virtual Screening Tools.[59] The grid center points were set to X = − 36.6352, Y = − 22.1218, Z = 55.6026, and the dimension (Å) X = 57.40, Y = 55.69, Z = 41.11. The grid box dimensions were selected and set up to wrap the protein's substrate-binding region. The BIOVIA Discovery Studio Visualizer 2017 was used to analyze the non-covalent interaction between the ligands and the pathogenic protein.[60]

2.5. ADMET Properties

ADMET parameters are mainly obtained to analyze the pharmacokinetic properties of medicinal compounds. Absorption, Distribution, Metabolism, Excretion, and Toxicity (ADMET) parameters of our reported 10 biological active compounds were collected from an online Database is called admetSAR (http://lmmd.ecust.edu.cn/admetsar2), which is the most trusted database for predicting the AMDET parameters Substrate.[61-63] We have focused on the ADMET parameters such as Plasma Protein Binding, Human Intestinal Absorption, Caco-2 Permeability, Blood-Brain Barrier, Renal Organic Cation Transporter, CYP450 2C9.

2.6. Calculation of QSAR and pIC_{50}

QSAR and pIC_{50} values were calculated with the help of the Chemdesk website and a standard equation of multiple linear regression (MLR) for QSAR and pIC_{50}. From this online database, eight most acceptable biochemical descriptors, such as Chiv5, bcutm1, MRVSA9, MRVSA6, PEOEVSA5, GATSv4, J and Diametert.[64]

3. Results and Discussions

3.1. Chemistry

D-Glucofuranose and its derivatives are considered very common compounds of carbohydrates as glucose group and have antibacterial and antifungal properties. Therefore,glucofuranose (1,2-*O*-isopropylidene protected) has been taken to this study. The most conceivable goal of this study is to examinethe effect of changing the D-glucofuranose side chain at the C-6 position on their antimicrobial activity. As it can be seen from Figure 1 below, an -OH is converted to phenyl ether at the C-6 position of the parent D-glucofuranose (**01**) forming6-*O*-phenyl-D-glucofuranose derivative (**02**).This benzene was later combined with eight different functional groups to form compounds **03-10**. With the help of molecular modelling, the computational chemistry tools of these compounds have been executed through specific studies of specific pathogens(black and white fungus) with proteins using molecular docking, and molecular dynamics tools. From the molecular docking study, it is illustrated how these D-glucofuranose derivatives combine with the protein of black and white fungus that is the main goal of this study.It has also been shown that bonds are formed for a functional group of D-glucofuranose and its derivatives to help neutralize protein pathogens, resulting in more pending affinity results for multiple bonds.

3.2. PASS Predication

Our reported molecules have shown the most potent antifungal activity, which is above Pa value 0.550+. Ligand no 03 and 10 showed the highest Pa value (Pa>0.618 & Pa>0.652) although the main focus is on the prediction of antifungal activity, considering some other prediction parameters, including antiviral, antibacterial, antibiotic, and cytotoxic activity, indicated that antibacterial and antifungal Pa value is much better. For antivirals, the highest Pa value is reported 0.452 in Ligand no **01,** whereas antibacterial has shown 0.563 is the highest the Pa> value in ligand no **07**&**09**. Among them, the PASS prediction value is much higher against fungi compared

to antiviral, antibacterial, antibiotic, and cytotoxic activity. So, these values indicate that the drugs candidate molecules will show strongactivity against the black and white fungus.

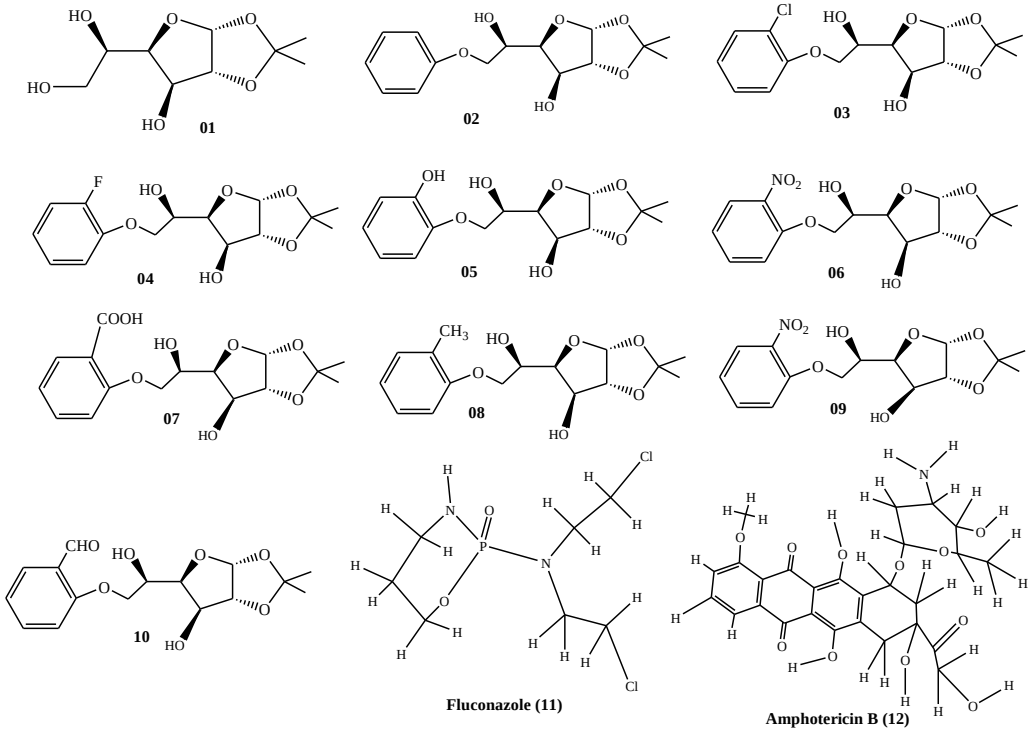

Figure 1. Molecular structure of the tested compounds

Table 1. Data of PASS prediction

Ligands	Antiviral		Antibacterial		Antifungal		Antibiotic		Cytotoxic	
	Pa	Pi	Pa	Pi	Pa	Pi	Pa	Pi	Pa	Pi
01	0.452	0.018	0.537	0.013	0.599	0.019	0.352	0.010	0.158	0.094
02	0.198	0.190	0.510	0.015	0.587	0.020	0.283	0.016	0.153.	0.098
03	0.354	0.154	0.474	0.019	0.618	0.017	0.224	0.015	0.127	0.126
04	0.360	0.054	0.501	0.016	0.532	0.026	0.255	0.019	0.127	0.126
05	0.434	0.023	0.529	0.014	0.597	0.019	0.293	0.015	0.381	0.078
06	0.296	0.234	0.523	0.014	0.579	0.021	0.275	0.017	0.173	0.084
07	0.081	0.072	0.563	0.011	0.587	0.020	0.323	0.012	0.131	0.121
08	0.403	0.034	0.500	0.016	0.585	0.020	0.006	0.004	0.140	0.110
09	0.363	0.053	0.563	0.011	0.587	0.020	0.323	0.012	0.131	0.121
10	0.406	0.033	0.510	0.015	0.652	0.013	0.276	0.017	0.155	0.096

3.3. Lipinski Rule, Pharmacokinetics and Drug Likeness

The typical assumption for the drug-likeness obtained from Lipinski's five-rule is commonly investigated.[65] In this section, all the drug candidate compounds have fulfilled the expected criteria and this section also investigated that the drug candidate has overall good bioavailability with high human intestinal absorption (HIA) (Table 2). The molecular value ranges of reported compounds are 220-342 g/mol and the lower molecular weight is reported 220.22 g/mol, where the higher molecular value is 342.31 g/mol. The topological surface area (TPSA) range was found between 77–123 (Å²). Overall these findings fully obeyed the Lipinski rule. As these reported compounds have high bioavailability, high GI absorption rate, as well as followed Lipinski rule, so we reached a decision that these all compounds are human usable.

Table 2. Data of Lipinski rule, pharmacokinetics and drug likeness

ligands	NBR	HBA	HBD	TPSA, Å²	Log Po/w Consensus	Log Kp (skin permeation), cm/s	Lipinski rule Result	Lipinski rule Viol.	M.W.	Bioavailability Score	GI absorption
01	2	6	3	88.38	-0.54	-7.84	Yes	0	220.22	0.55	High
02	4	6	3	77.38	1.07	-7.17	Yes	0	296.32	0.55	High
03	4	6	2	77.38	1.60	-6.93	Yes	0	330.76	0.55	High
04	4	7	2	77.38	1.34	-7.21	Yes	0	314.31	0.55	High
05	4	7	3	97.61	0.74	-7.52	Yes	0	312.32	0.55	High
06	5	8	2	123.20	0.25	-7.57	Yes	0	341.31	0.55	High
07	5	8	3	114.68	0.58	-7.77	Yes	0	340.33	0.56	High
08	4	6	2	77.38	1.50	-6.99	Yes	0	310.44	0.55	High
09	5	8	3	114.68	0.58	-7.77	Yes	0	340.33	0.56	High
10	5	7	2	94.45	0.79	-7.72	Yes	0	324.34	0.55	High

Viol: Violation

3.4. Optimized structure of D-glucofuranose and its derivatives

Figure 2 represents the optimized chemical structures of D-glucofuranose and its derivatives which have been simulated by computational techniques using the DFT method. It is well revealed that the optimized structure carries the symmetry and asymmetry point through the molecules, which has to contribute to the forming of chemical properties as well as biological significance with perfect configuration.

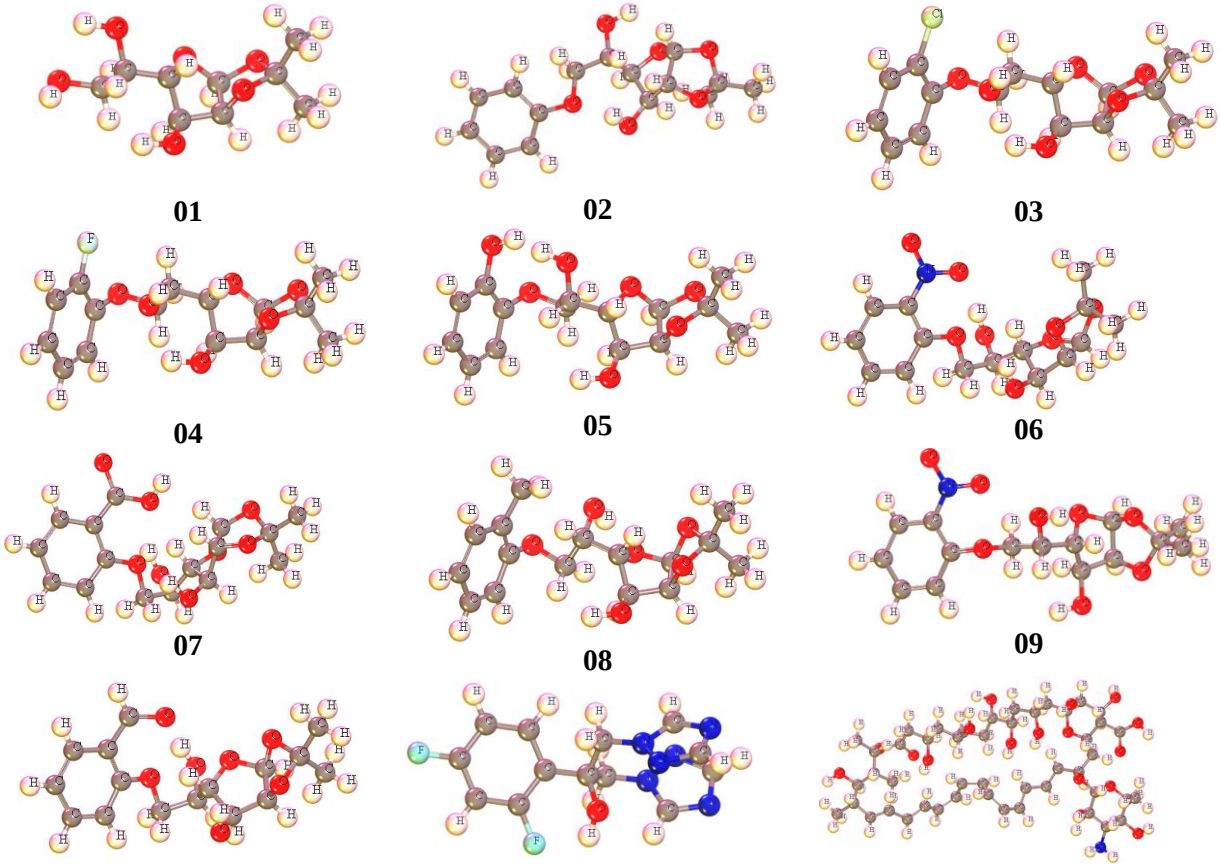

Figure 2. Optimized structure of molecules

3.5. Chemical Descriptors

The word HOMO belongs to the highest occupied molecular orbital, whereas LUMO illustrates the lowest unoccupied molecular orbital. With the help of the DFT method, the energies of HOMO and LUMO have been measured. Energy gaps of frontier molecular orbitals are used to assess atomic electrical transport characteristics. For good chemical stability, it is necessary to have a broad HOMO-LUMO distance, and a narrow HOMO-LUMO gap represents the higher atomic system, and lower chemical stability because they are the closest to each other. From Table 3, the energy gap is about -8.00 kcal/mol which indicates the lower atomic system and higher chemical stability for each molecule but it slightly changes with respect to changing the functional groups.

Bioactivity can be described by the chemical potential (m), hardness (h), softness (S), and electrophilicity coefficient.[66,67] The positive chemical potential discloses the stability of the systems.The general magnitude of hardness is greater than the softness of the compound, which indicates that the molecules convey high biochemical stability. It is recorded that the hardness isabout -4.00 kcal/mol. All the values of chemical potentials have been obtained positively, which indicates reinforcement to the stability. The results are summarized below (Table 3). This evidence can play a crucial role in the bioactivity of the compound.

In this study, compound **8** has the HOMO-LUMO largest gap of 8.667 eV whereas compound **6** shows the lowest energy gap (7.38 eV) and the lowest chemical potential (-3.7252 eV) with the highest chemical softness (0.9986 eV) values which may contribute to the higher chemical reactivity than others.

Table 3. Data of chemical descriptors

Ligands	**A=-LUMO**	**I=- HOMO**	**E GAP=I-A**	**Chemical potential** $(\mu) = -\frac{I+A}{2}$	**Electronegativity:** $(\chi) = \frac{I+A}{2}$	**Hardness:** $(\eta) = \frac{I-A}{2}$	**Softness** $(\sigma) = \frac{1}{\eta}$	**Electrophilicity:** $(\omega) = \frac{\mu^2}{2\eta}$
01	-2.492	-10.08	7.590	6.287	-6.287	-3.795	-0.2635	-5.2077
02	-0.103	-8.121	8.018	4.112	-4.112	- 4.009	- 0.2494	- 2.1088
03	-0.126	-8.736	8.610	4.431	-4.431	-4.305	-0.2323	-2.2803
04	-0.176	-8.803	8.627	4.489	-4.489	-4.313	-0.2318	-2.3363
05	-0.51	-9.173	8.663	4.841	-4.841	-4.331	-0.2309	-2.7058
06	-2.286	-9.672	7.386	5.979	-5.979	-3.693	-0.2708	-4.8400
07	-1.513	-9.439	7.926	5.476	-5.476	-3.963	-0.2523	-3.7833
08	-0.030	-8.697	8.667	4.363	-4.363	-4.333	-0.2308	-2.1969
09	-2.181	-9.729	7.926	5.955	-5.955	-3.774	-0.2649	-4.6982
10	-1.149	-8.989	7.840	5.069	-5.069	-3.920	-0.2551	-3.2774
11	-9.052	-1.238	7.814	5.145	-5.145	-3.907	-0.2560	-3.3876
12	-0.778	-6.781	6.003	3.779	-3.779	-3.001	-0.3332	-2.3796

3.6. Frontier Molecular Orbitals (HOMO and LUMO)

HOMO and LUMO are superior catalysts regulating the chemical properties of any chemical compound by which all their chemical properties are determined and controlled. In this context, the chemical properties of designed derivatives have been predicted. Since these compounds contain oxygen atoms in addition to the aromatic ring and heterocyclic ring, it is still difficult to find an alternative to the HOMO and LUMO diagram to clearly understand whether the aromatic chain or heterocyclic ring controls the chemical properties.[68-73] As it can be seen from the picture shown in Figure 3 (the deep maroon and yellow of LUMO are positive and negative ends of the orbital node, respectively, and lime and orange color are for positive and negative ends of the orbital node, respectively), there is a very subtle difference between HOMO and LUMO. HOMO, on the other hand, is similarly extended just above the benzene ring, although this extent is less than that of HOMO, and no effect can be observed on the benzene ring and chain. But the LUMO is illustrated through the benzene ring, as well as the side chain. Not to mention that after adding benzene, their orbitals (HOMO and LUMO) are not found in any part of the furanose

ring as acting the functional group, so it is clear that benzene and the associated site chain control the chemical behavior of these compounds.

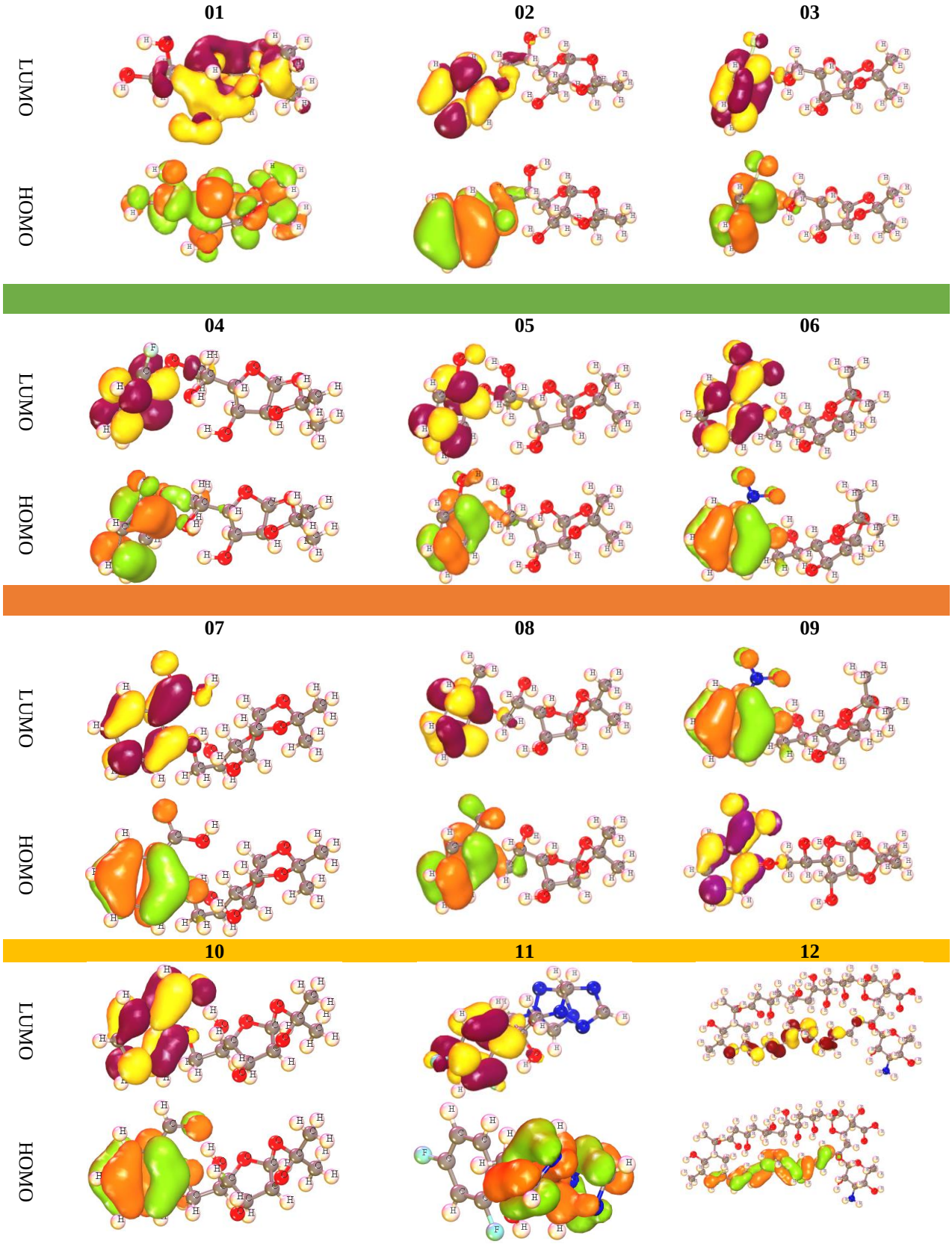

Figure 3. HOMO-LUMO diagram of the reported compounds

3.7. Map of Electrostatic Potential (MEP) Charge Distribution

The MEP map is a helpful tool for determining how a molecule's total charges (positive and negative) are dispersed across the molecule. In addition, it can determine the presence of ligands or protein binding regions, as well as suitable sites for an electrophilic attack site or nucleophilic attack site. The nucleophilic and electrophilic sites of the compounds can be obtained by the molecular electrostatic potential MEP. Below Figure 4, the positive electrostatic potential regions have been highlighted in blue color (electrophilic site), whereas the red color represents the nucleophilic attack region. The positive charges areas are observed to be significantly greater compared to the negative charge region, which indicated that, the electrophilic groups in these molecules are more attracted to nucleophilic.

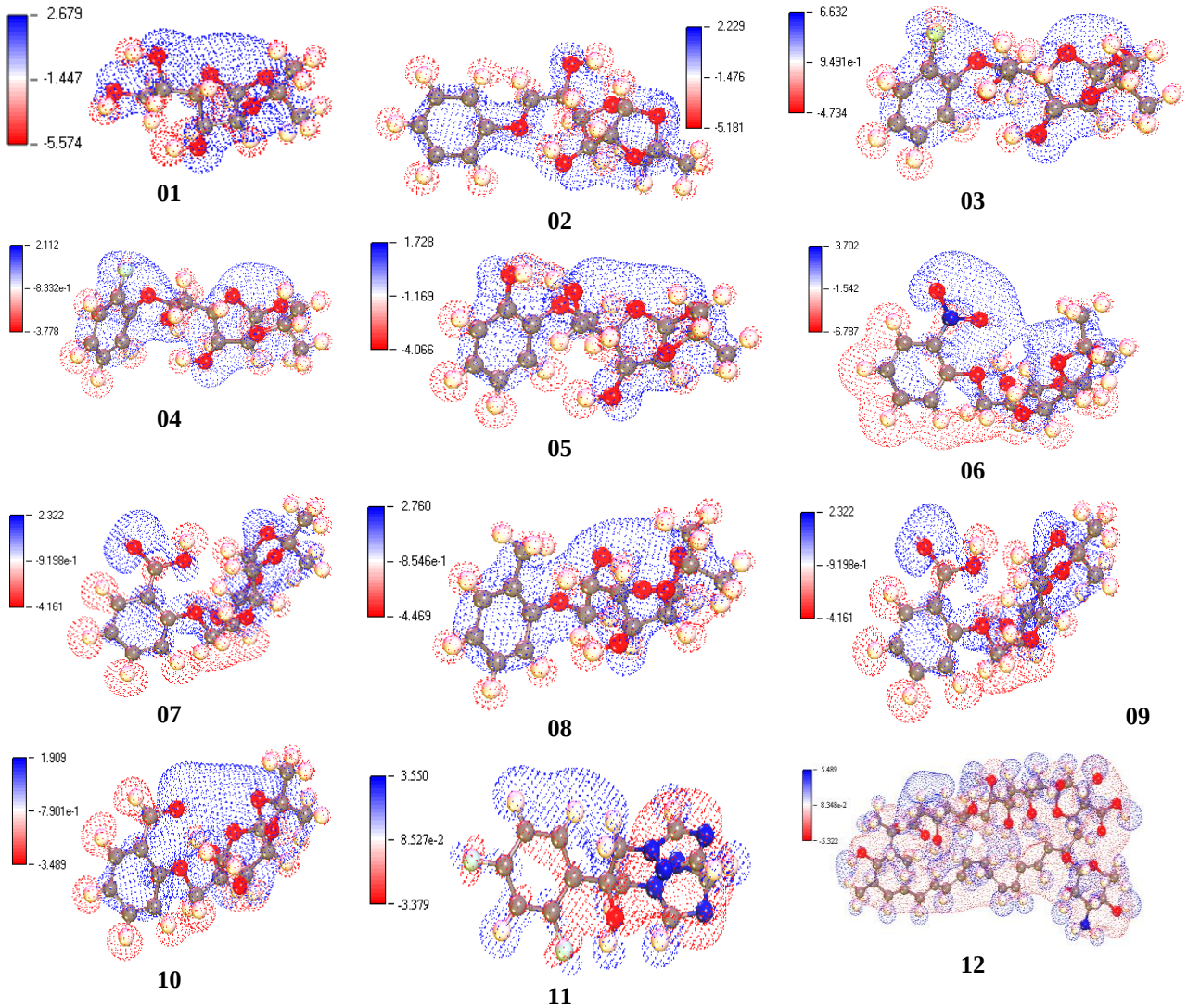

Figure 4. Map of Electrostatic Potential (ESP)charge distribution of the reported compounds

3.8. Molecular Docking Against Black Fungus

As the recognized binding energy is about -6.0 kcal/mol for standard drugs [74-78] and the selected drug candidate molecules against black fungus proteins of *Mycolicibacterium smegmatis* (7D6X), *Mucor lusitanicus*(6ZDW), and *Rhizomucor miehei*(6ZDW) have shown a good and strongest binding affinity. When the overall binding affinity was investigated, it is seen that D-glucofuranose and its derivatives have much more effectiveness including better binding affinity against these three fungal proteins. Among them, the largest binding affinity was recorded at -9.4 kcal/mol against 7D6X in ligand no **07**, -7.5 kcal/mol was recorded against 6ZDW in Ligand no **06** and **07**, and -7.8 kcal/mol was recorded against *Rhizomucor miehei* in ligand no **07** (Table 4).

Table 4. Data of molecular docking against black fungus pathogens

	***Mycolicibacterium smegmatis* (7D6X)**			***Mucor lusitanicus* (6ZDW)**			***Rhizomucor miehei* (4WTP)**		
L/N	**Binding Affinity (kcal/mol)**	**No of H bond**	**No of Hydrophobic bond**	**Binding Affinity (kcal/mol**	**No of H bond**	**No of Hydrophobic bond**	**Binding Affinity (kcal/mol**	**No of H bond**	**No of Hydrophobic bond**
01	-7.0	03	02	-5.4	01	01	-6.4	04	01
02	-7.6	05	05	-7.0	01	02	-7.4	03	07
03	-7.5	02	07	-6.6	01	02	-7.7	02	08
04	-7.5	09	02	-6.7	03	01	-7.6	01	07
05	-7.4	06	03	-6.9	01	01	-7.5	02	07
06	-8.0	05	06	-7.5	03	01	-73	03	07
07	-9.4	03	04	-7.5	02	01	-7.8	02	07
08	-8.8	02	04	-6.7	01	02	-7.7	04	10
09	-8.3	02	03	-7.0	03	01	-7.7	05	08
10	-8.7	03	03	-7.1	03	01	-7.4	01	07
11	-7.2	05	03	-7.2	02	02	-7.0	03	03
12	-8.4	02	01	-8.3	03	00	-10.5	04	04

3.9. Molecular Docking Against White Fungus

The excellent binding affinity against black fungus has been illustrated in Table 5. The selected three white fungus proteins such as *Candida Auris*(6U8J), *Aspergillus luchuensis* (1BK1), and *Candida albicans* (5HW7) have performed the docking to complete this research work more broadly and to see if the designed drugs would work against white fungus or what kind of binding affinity was available against white fungus. The most acceptable outcome from designing drugs also has a better binding affinity against white fungus than black fungus from Table 4 and Table 5. Our finding has obtained the highest binding affinity -8.5 kcal/mol against *Aspergillus luchuensis*. Since the standard value or binding energy of a potential drug is almost -6.0 kcal/mol[74] and all the designing compounds cross this standard value excluding ligand no **01** against *Candida albicans* (5HW7).

Table 5. Data of molecular docking against white fungus pathogens

	***Candida Auris* (6U8J)**			***Aspergillus luchuensis* (1BK1)**			***Candida albicans* (5HW7)**		
L/N	**Binding Affinity (kcal/mol)**	**No of H bond**	**No of Hydrophobic bond**	**Binding Affinity (kcal/mol**	**No of H bond**	**No of Hydrophobic bond**	**Binding Affinity (kcal/mol**	**No of H bond**	**No of Hydrophobic bond**
01	-6.4	06	04	-6.4	03	05	-5.6	04	01
02	-6.7	05	03	-8.5	01	07	-6.9	01	05
03	-7.4	04	02	-8.4	01	07	-6.6	00	05
04	-7.1	04	03	-8.4	02	08	-7.0	02	04
05	-8.1	05	05	-8.0	03	06	-7.3	02	07
06	-6.6	06	03	-8.1	03	06	-7.0	05	04
07	-7.0	05	03	-8.4	03	06	-6.8	03	03
08	-6.8	01	07	-8.5	02	09	-7.1	01	10
09	-7.2	06	02	-8.1	06	07	-6.6	03	05
10	-6.7	05	03	-8.3	05	01	-7.0	03	04
11	-7.0	05	05	-7.6	05	06	-6.3	02	01
12	-7.5	05	00	-8.3	05	00	-8.2	01	04

3.10. Protein-Ligands Interaction and Active Sites Binding by Docking

There are two types of bonds, such as hydrophobic bonds and hydrogen bonds which occur between ligands and protein. As it is observed that compound **07** (Figure 5) conveys the highest binding score in protein by docking. For compound **07** against *Mycolicibacterium smegmatis*, the binding sites are at LYS-39(1.95298), SER-40 (2.62951), GLY-15 (3.74059) as hydrogen bonds and LEU-432 (4.07746), HIS-46 (4.85362), LYS-39(5.26593) as the hydrophobic bond and other interaction shown in Table S01, S02, and S03.

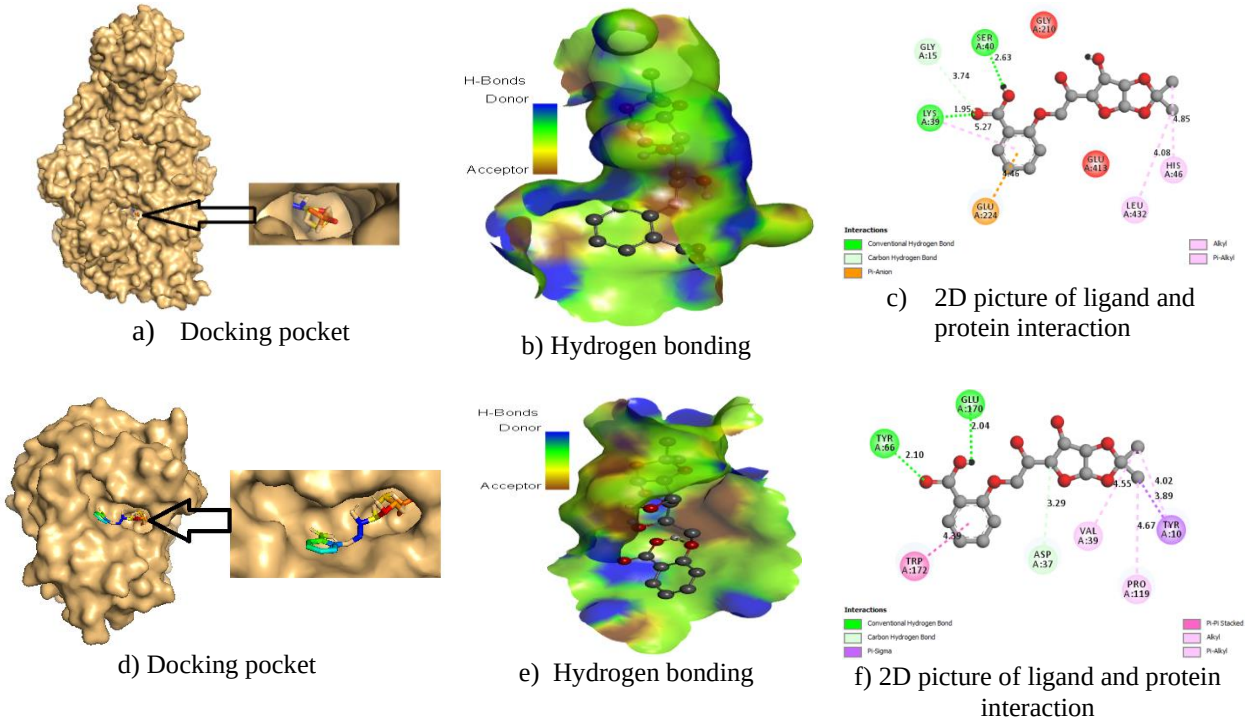

a) Docking pocket

b) Hydrogen bonding

c) 2D picture of ligand and protein interaction

d) Docking pocket

e) Hydrogen bonding

f) 2D picture of ligand and protein interaction

Figure 5. Different docking poses of **07** sample against *Mycolicibacterium smegmatis* and *Aspergillus luchuensis*

3.11. Molecular Dynamics

The molecular dynamics is a boulevard for trying the accuracy docking procedure in the prospect of the root-mean-square deviation (RMSD) and root-mean-square fluctuation (RMSF) which provide in rank about their binding pose ligand-protein complex after docking. It is divulged that the RMSD of the docking complex is less than 2 Å for becoming a good fitting pose of Ligand in drug pocket and software can accurately dock the ligand-protein complex.[79]Molecular docking score showed docked complexes that the compound **07** and **08** with the highest binding score against black fungus protein. Besides the standard **12** showed the top binding score as standard for black fungal infection. That is why in this study molecular dynamics was performed for only **07**, **08**, and **12**. The molecular dynamics were analyzed for time versus protein chain where there is no interaction with the protein shown in Figure 6. It is observed that the RMSD is below 1.1 Å. After interacting with the backbone, it is similar to the previous picture.

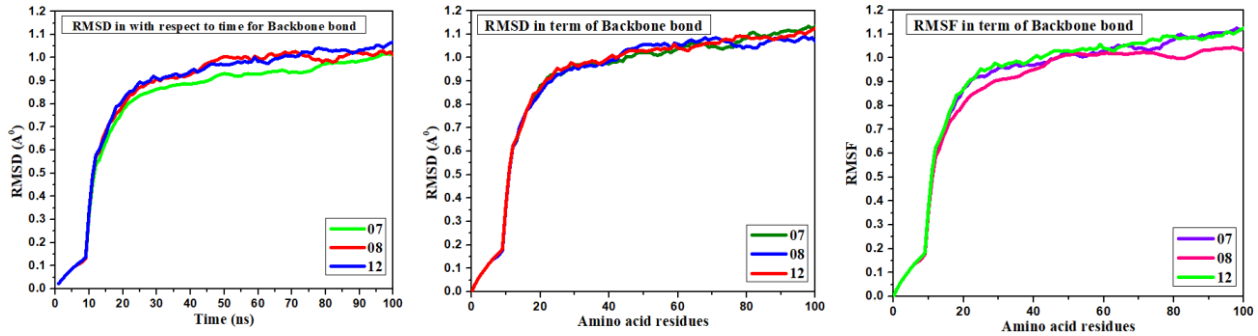

RMSD: Time vs protein skeleton b) RMSD: Amino acid vs backbond c) RMSF: Amino acid vs backbond

Figure 6. Various picture of RMSD and RMSF for protein (7d6x)

On the other hand, the RMSF is observed that there is a use fluctuation after time period 50 ns which are higher for **07** and the low fluctuation is observed for **08** and **12** in case of time vs protein skeleton as shown in Figure 7.

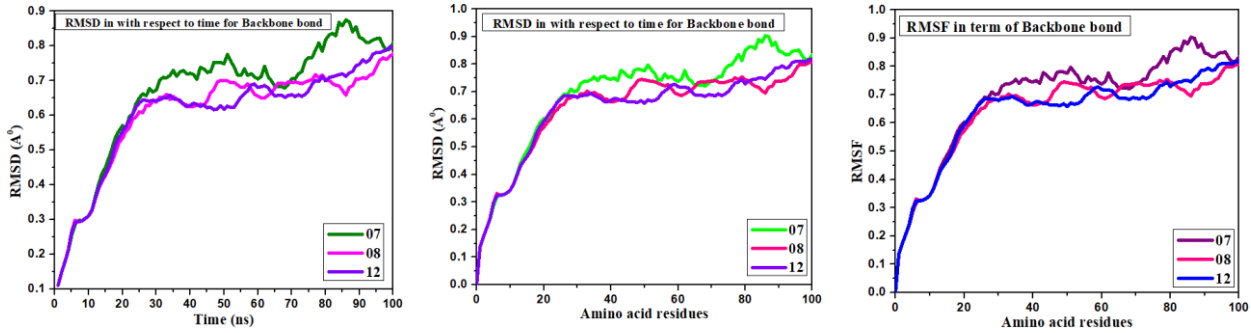

RMSD: Time vs protein skeleton b) RMSD: Amino acid vs backbond c) RMSF: Amino acid vs backbond

Figure 7. Various picture of RMSD and RMSF for protein (1BK1)

3.12. ADMET Properties and Aquatic and Non-aquatic Toxicity

The characteristics of a new drug candidate or any therapeutic agent like absorption, distribution, metabolism, elimination, or toxicity (ADMET) are the most important parameters or factors. The chemical ADMET parameter has been obtained from admetSAR including; human intestinal absorption (HIA), blood-brain barrier (BBB), Caco-2 Permeability, etc. attached in Table 6. Our designed all drugs have provided excellent GI absorption, positive of BBB+ except **06**, positive to P-I glycoprotein inhibitor, negative response in Renal Organic Cation Transport, CYP4502C9 Substrate, and CYP4501A2 Inhibitor. In addition, all of the compounds have to stay in Mitochondria, as well as the values of Human Intestinal Absorption and Caco-2 Permeability are slightly higher than moderate.

Table 6. Data for ADME parameters

S/N	Human Intestinal Absorption	Caco-2 Permeability	Blood Brain Barrier	P-I glycoprotein inhibitor	P-II glycoprotein substrate	Renal Organic Cation Transporter	Sub-cellular localization	CYP450 2C9 Substrate	CYP450 1A2 Inhibitor
01	0.5952	0.7302	BBB+	No	Yes	No	Mitochondria	No	No
02	0.8026	0.6128	BBB+	No	Yes	No	Mitochondria	No	No
03	0.7840	0.5500	BBB+	No	Yes	No	Mitochondria	No	No
04	0.7847	0.5540	BBB+	No	Yes	No	Mitochondria	No	No
05	0.9482	0.6025	BBB+	No	Yes	No	Mitochondria	No	No
06	0.5567	0.5899	BBB-	No	No	No	Mitochondria	No	Yes
07	0.8371	0.6397	BBB+	No	Yes	No	Mitochondria	No	No
08	0.6765	0.6020	BBB+	No	Yes	No	Mitochondria	No	No
09	0.8371	0.6397	BBB+	No	Yes	No	Mitochondria	No	No
10	0.8371	0.6397	BBB+	No	Yes	No	Mitochondria	No	No

On the other hand, aquatic and non-aquatic toxicity has been reported for all drugs shown in Table 7. It is found that all drugs are non-carcinogenic, non-responder to AMES toxicity without **06**, intermediate water-soluble which is found the highest in **03**, indicating the functional groups can be acted to reduce the water solubility, as a result, lead the low toxicity for both the aquatic and non-aquatic environment and its composition after use or extracted from human body after doses. The different compounds have shown different acute oral toxicity and their value range is recorded 2.168 kg/mol to 2.850 kg/mol. *T. Pyriformis* toxicity is also reported positive and only Ligand no **01** has shown negative value.

Table 7. Aquatic and non-aquatic toxicity

S/N	AMES toxicity	Carcinogenicity	Water solubility, Log S	Plasma protein binding	Acute Oral Toxicity, kg/mol	Oral Rat Acute Toxicity (LD50) (mol/kg)	Fish Toxicity pLC50 mg/L	*T. Pyriformis* toxicity (log ug/L)
01	No	No	-0.801	0.179	2.464	1.9593	2.4984	-0.6809
02	No	No	-2.064	0.951	2.168	2.5058	1.061	0.1795
03	No	No	-3.097	1.231	2.850	2.7886	0.4593	0.5871
04	No	No	-2.86	1.191	2.582	2.8900	0.5698	0.5359
05	No	No	-2.143	0.993	2.347	2.5309	0.8951	0.3867
06	Yes	No	-2.949	1.012	2.569	2.6449	1.0354	0.7324
07	No	No	-2.029	0.986	2.559	2.6974	0.6775	0.4923
08	No	No	-2.710	1.166	2.238	2.7747	0.9953	0.5980
09	No	No	-2.029	0.986	2.559	2.6974	0.6775	0.4923
10	No	No	-2.090	0.926	2.209	2.6974	0.6775	0.4923

3.13. Calculation of QSAR and pIC$_{50}$

Quantitative structure activities relationship (QSAR) calculation has been performed to determine the relationship between biological activities and structural activities of chemical compounds using computational methods.utilizing the multiple linear regression (MLR) equation, the QSAR model has been carried out. The overall value of QSAR and pIC$_{50}$ investigation meets all the criteria and it is observed that different compounds have different QSAR and pIC$_{50}$. It is found the range of QSAR and pIC$_{50}$ is between 4.77 and 4.33 where the higher value of QSAR and pIC$_{50}$ is at 4.77 and the lower value is found at 4.33. The estimated pIC$_{50}$ (Table 8) suggests that these reported compounds might be biologically useful against fungi.

Here, pIC50 (Activity) = − 2.768483965 + 0.133928895 × (Chiv5) + 1.59986423 × (bcutm1) + (− 0.02309681) × (MRVSA9) + (− 0.002946101) × (MRVSA6) + (0.00671218) × (PEOEVSA5) + (− 0.15963415) × (GATSv4) + (0.207949857) × (J) + (0.082568569) × (Diametert)

Table 8. Data of QSAR parameters

SL. No.	Chiv5	(bcutm1)	(MRVSA9)	(MRVSA6)	(PEOEVSA5)	GATSv4	J	Diametert	PIC50
01	1.231	3.828	0.000	0.000	0.000	1.029	2.046	8.0	4.33
02	1.718	3.844	0.000	30.332	18.199	1.069	1.485	12	4.77
03	1.84	3.941	11.601	29.288	23.734	1.018	1.501	12	4.73
04	1.73	3.851	0.000	30.083	12.133	1.103	1.501	12	4.74
05	1,74	3.852	0.000	24.265	12.133	1.100	1.501	12	4.76
06	0.336	3.874	5.687	34.38	12.133	1.072	1.516	12	4.46
07	1.856	3.868	5.969	29.829	12.133	1.011	1.516	12	4.67
08	1.823	3.856	0.000	29.829	18.199	1.018	1.501	12	4.82
09	1.856	3.868	5.969	29.829	12.133	1.011	1.516	12	4.67
10	1.819	3.862	6.286	29.829	12.133	1.013	1.503	12	4.64

The computational screening of inhibitor for black fungus and white fungus

3.14. Comparative Study of Docking Score Between Ketal and Non-ketal Form of Molecules

Glucofuranoses **01**-**10**are in ketal form (with 1,2-*O*-isopropylidene group) and are moderately stable as the anomeric position is involved in the acetonide group. However, under theacidic condition, the acetonide group undergo ring-opening as shown below (Scheme 1).

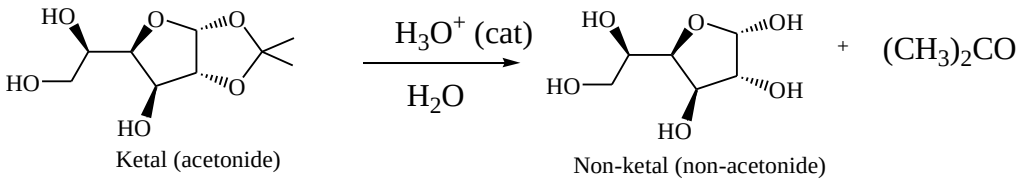

Scheme 1. Interconversion between acetonide and non-acetonide forms of D-glycofuranose

In the present investigation, molecular docking has been performed for **01**-**10** having acid-sensitive acetonide group, which may open under biological condition(s). Thus, for comparison and validation, three non-acetonide glucofuranoses (NK01, NK02, and NK03; Figure 8) corresponding to **01**-**03** are also performed for molecular docking.

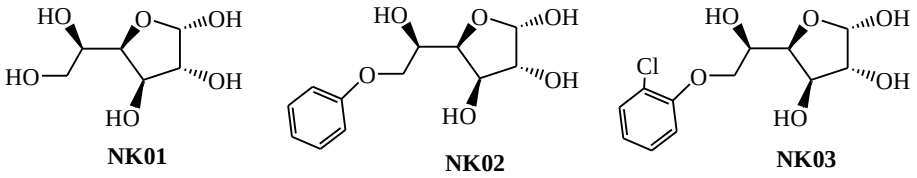

Figure 8. Molecular structure of **NK01**-**NK03** (non-ketal form).

For comparison, **NK01**-**NK03** have been docked with both the black and white fungal strain to evaluate the binding affinity. The results are compared with the results of the ketal form attached in Figure 9 through the bar diagram. In the case of black fungus, the binding affinity of non-ketal compounds is higher than non-ketal form, and it is obtained a similar result for white fungus protease.

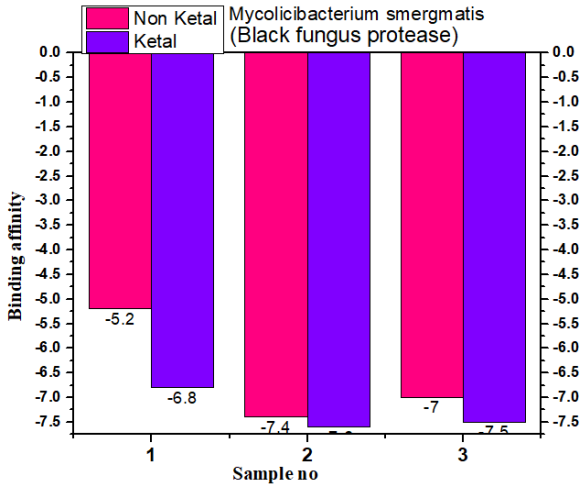

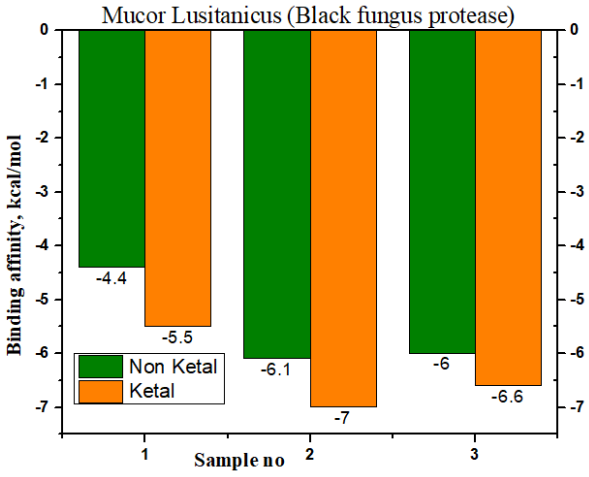

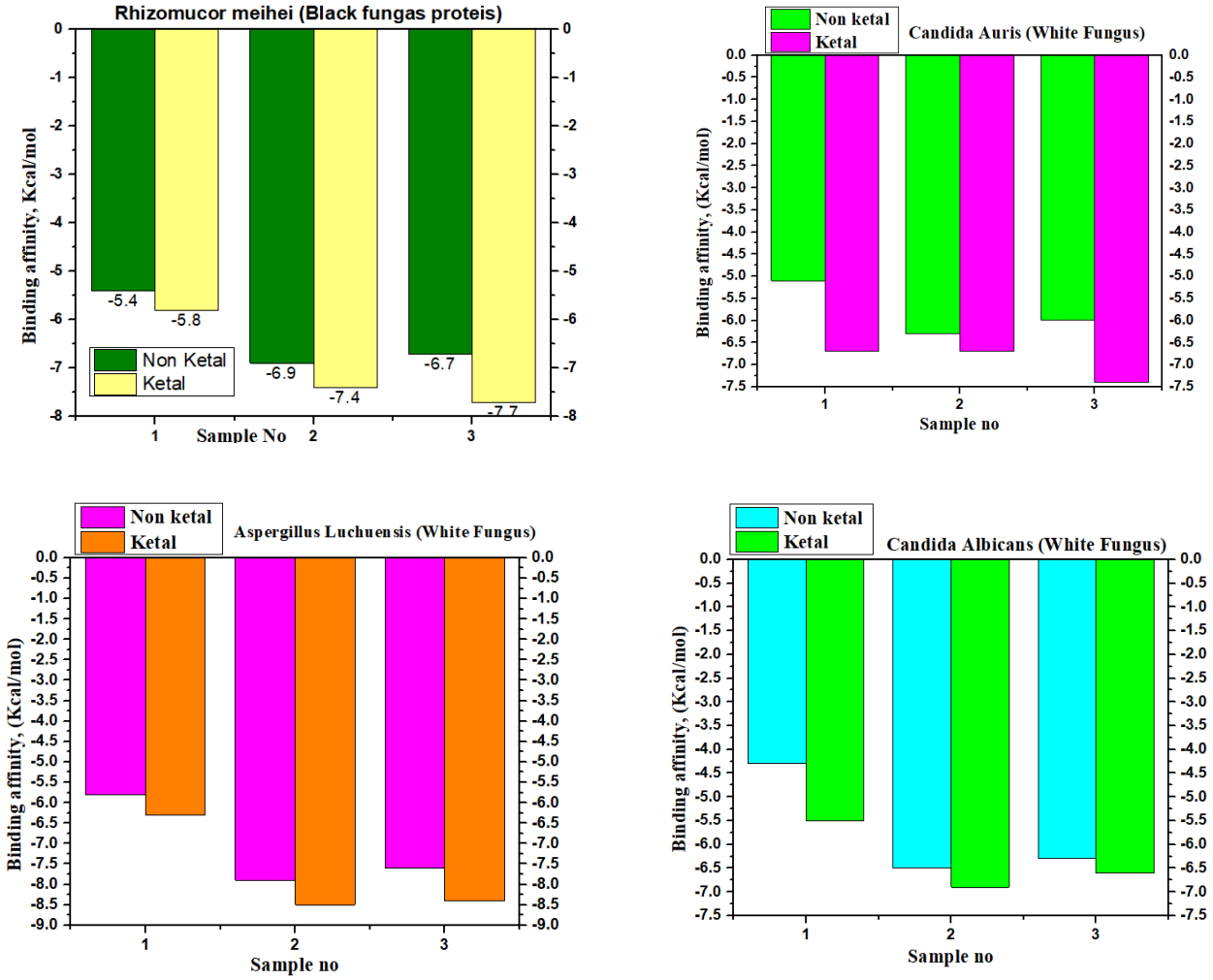

Figure 9. Comparative study of docking score between ketal and non-ketal form

4. Conclusion

The computational investigations have been performed against both black and white fungus using the D-glucofuranose and its derivatives, where the molecular modeling from computational tools has been executed to design new functionalized molecules. The PASS prediction proposed their slightly antifungal activity rather than other pathogens. To get more authentic exploration, molecular docking has been performed against both black and white fungus, calculating the binding affinity. Regarding that scale, the highest docking score is recorded at -9.4 kcal/mol against *Mycolicibacterium smegmatis*(7D6X), a black fungus pathogen strain, whereas the binding affinity -8.5 kcal/mol is obtained as the highest binding energy against *Aspergillus luchuensis* **(**1BK1), a white fungus. It must be noted that the used standard drugs, **11**, **12,** convey -7.2 and -8.4 against *Mycolicibacterium smegmatis, and* -7.6 and -8.3 binding affinity against *Aspergillus luchuensis* **(**1BK1). However, it could be concluded that the tested drugs would be able to show a higher binding affinity rather than standard anda similar case for molecular dynamic accounting for RMSD and RMSF. Into the bargain, the potential drug candidates are also shown overall a better pharmacokinetics parameter, non-carcinogenic, low solubility in water, satisfied the Lipinski rule and drug-likeness properties. Finally, it might be said that the D-glucofuranose and its derivatives are more effective in black fungus than white fungus protein, and the carboxylate group (**07**) and methyl group (**08**) are highly responsible for conveying the higher binding affinity (-9.4 and -8.8, kcal/mol, respectively) against black fungus. At the same time,compounds **02** and **08** showed the highest binding affinity against white fungus, and **0**3, **04**, and **07** are in the second position. They have been proved that the carboxylic group proliferates the binding affinity for both black and white fungus protein.

Acknowledgements

Authors acknowledge to the European University of Bangladesh, Gabtoli, Dhaka-1216, Bangladesh and University of Chittagong, Bangladesh.

ORCID

Ajoy Kumer: 0000-0001-5136-6166
Unesco Chakma: 0000-0003-1711-7216
Mohammed M. Matin: 0000-0003-4965-2280
Shopnil Akash: 0000-0003-1751-705X
Akhel Chandro: 0000-0002-6076-8383
and Debashis Howlader: 0000-0003-4149-971X

References

[1] Shoham, S.L.; Stuart M. The immune response to fungal infections. *Br. J. Haematol* **2005**,*129*, 569-582.
[2] Dean, D.A.; Burchard, K.W. Fungal infection in surgical patients. *Am. J. Surg.* **1996**, *171*, 374-382.
[3] Brown, J. Zygomycosis: an emerging fungal infection. *Am. J. Health Syst. Pharm* .**2005**, *62*, 2593-2596.
[4] Alonso, R.; Pisa, D.; Marina, A.I.; Morato, E.; Rabano, A.; Carrasco, L. Fungal infection in patients with Alzheimer's disease. *J. Alzheimer's Dis* .**2014**, *41*, 301-311.
[5] Foster, K.W.; Ghannoum, M.A.;Elewski, B.E. Epidemiologic surveillance of cutaneous fungal infection in the United States from 1999 to 2002. *JAAD*, **2004**, *50*, 748-752.
[6] Li, Z.; Lu, G.; Meng, G. Pathogenic fungal infection in the lung. *Front. Immunol.* **2019**,*10*, 1524.
[7] Caston-Osorio, J.; Rivero, A.; Torre-Cisneros, J. Epidemiology of invasive fungal infection. *Int. J. Antimicrob.* **2008**,*32*, S103-S109.
[8] Barnes, R.A. Early diagnosis of fungal infection in immunocompromised patients. *J. Antimicrob. Chemother*, **2008**, 61, i3-i6.
[9] Mirsky, H.S. Cuttner, J. Fungal infection in acute leukemia. *Cancer*, **1972**, *30*, 348-352.
[10] Kubak, B. Fungal infection in lung transplantation. *Transplant Infect. Diseas.* **2002**, *4*, 24-31.
[11] Fung, J. Fungal infection in liver transplantation. *Transplant Infect. Diseas.* **2002**, *4*, 18-23.
[12] Krasinski, K.;Holzman, R.S.; Hanna, B.; Greco, M.A.; Graff, M.; Bhogal, M. Nosocomial fungal infection during hospital renovation. *Hosp. Epidemiol.* **1985**, *6*, 278-282.
[13] Nosari, A.; Oreste, P.; Montillo, M.; Carrafiello, G.; Draisci, M.; Muti, G.; Molteni, A.; Morra, E. Mucormycosis in hematologic malignancies: an emerging fungal infection. *Haematologica* **2000**, *85*, 1068-1071.
[14] Rawson, T.M.; Wilson, R.C., Holmes, A. Understanding the role of bacterial and fungal infection in COVID-19.*Clin Microbiol Infect*. **2021**, *27*, 9.
[15] Li, C.-S.; Pan, SF. Analysis and causation discussion of 185 severe acute respiratory syndrome dead cases.*Zhongguo Wei Zhong Bing Ji Jiu Yi Xue*. **2003**, *15*(10), 582-584.
[16] El-Kholy, N.A.; Abd El-Fattah, A. M.;Khafagy, Y.W. Invasive fungal sinusitis in post COVID-19 patients: a new clinical entity. *The Laryngoscope* **2021**,*131*(*12*), 2652-2658.
[17] Chen, N.; Zhou, M.; Dong, X.; Qu, J.; Gong, F.; Han, Y.; Qiu, Y.; Wang, J.; Liu, Y.; Wei, Y. Epidemiological and clinical characteristics of 99 cases of 2019 novel coronavirus pneumonia in Wuhan, China: a descriptive study. *Lancet* **2020**, *395*, 507-513.
[18] Cornely, O.A.; Alastruey-Izquierdo, A.; Arenz, D.; Chen, S.C.A.; Dannaoui, E.; Hochhegger, B.; Hoenigl, M.; Jensen, H.E. Global guideline for the diagnosis and management of mucormycosis: an initiative of the European Confederation of Medical Mycology in cooperation with the Mycoses Study Group Education and Research Consortium. *Lancet Infect. Dis* .**2019**,*19*, e405-e421.
[19] deShazo, R.D.; Chapin, K.; Swain, R.E. Fungal sinusitis, *New Engl. J. Med.* **1997**, *337*, 254-259.
[20] Sharma, S.; Grover, M.; Bhargava, S.; Samdani, S.; Kataria, T. Post coronavirus disease mucormycosis: a deadly addition to the pandemic spectrum. *J. Laryngol Otol.* **2021**, *135*, 442-447.
[21] Dyer, O. Covid-19: India sees record deaths as "black fungus" spreads fear. *British Med. J.* **2021**, *373*, n1238.
[22] Balwan, W.K. Epidemiology of Mucormycosis in India: A notifiable disease. *Saudi J. Pathol. Microbiol.* **2021**,*6*, 187-191.
[23] Jeong, W.K.; C; Wolfe, R; Lee, W Leng; Slavin, MA; Kong, DCM; Chen, SC-A. The epidemiology and clinical manifestations of mucormycosis: a systematic review and meta-analysis of case reports. *Clin. Microbiol. Infect*. **2019**, *25*, 26-34.

[24] Dismukes, W.E.; Pappas, P.G.;Sobel, J.D. *Clinical Mycology* **2003**, Oxford Univ. Press.
[25] Rahman, F.I.; Islam, M.R.; Bhuiyan, M.A. Mucormycosis or black fungus infection is a new scare in South Asian countries during COVID-19 pandemic: Associated risk factors and preventive measures. *J. Med. Virol*. **2021**, *93*, 6447-6448.
[26] Gambhir, R.S.; Aggarwal, A.; Bhardwaj, A.; Kaur, A.; Kaur, R.;Sohi, S.M. COVID-19 and mucormycosis (black fungus): an epidemic within the pandemic. *Rocz. Panstw. Zakl. Hig.* **2021**, *72*, 239-244.
[27] Krishnan, M. COVID: India's 'white fungus' infections raise new health concerns. 25 May 2021.
[28] Sahoo, J.P.; Bhagyalaxmi,P.; Prasad, M.; Samal, A.; Chandra, K. The unseen "Fungal Infections"–An extra thrust aggravating COVID second wave in India. *Biotica Rese. Today* **2021**, *3*, 354-356.
[29] Barnes, P.D.M.; Kieren A. Aspergillosis: spectrum of disease, diagnosis, and treatment. *Infect. Dis. Clin. North Am.* **2006**, *20*, 545-561.
[30] Biswas, S. 'White fungus': Drug-resistant fungal infections pose threat to India patients, *BBC News*.
[31] Schmiedel, Y.; Stephan, Z. Common invasive fungal diseases: an overview of invasive candidiasis, aspergillosis, cryptococcosis, and *Pneumocystis pneumonia*. *Swiss Med. Wkly*. **2016**,*146*, w14281.
[32] Leopardi, S.; Blake, D.;Puechmaille, S.J. White-nose syndrome fungus introduced from Europe to North America.*Curr. Biol.* **2015**, *25*, R217-R219.
[33] Berger, S.; Chazli, Y.L.; Babu, A.F.; Coste, A.T. Azole resistance in *Aspergillus fumigatus*: a consequence of antifungal use in agriculture? *Front. Microbiol.* **2017**, 7-*8*, 1024.
[34] Arendrup, M.C.; Patterson, T.F. Multidrug-resistant Candida: epidemiology, molecular mechanisms, and treatment. *J. Infect. Dis.* **2017**, *216*, S445-S451.
[35] Ashu, E.A.; Korfanty, G.A.; Samarasinghe, H.; Pum, N.; You, M.; Yamamura, D.; Xu, J. Widespread amphotericin B-resistant strains of *Aspergillus fumigatus* in Hamilton, Canada. *Infect. Drug Resis.* **2018**, *11*, 1549-1555.
[36] E-Paper. Black fungus: How infection starts, death rate, treatment, medicine & other key things to know. *The Economic Times* (May 28, 2021).
[37] Pattanayak, M. Amphotericin B not the only cure available for black fungus: ICMR, *Business Today.In* (Jun 04, 2021)
[38] Zhao, H.; Zong, G.; Zhang, J.; Wang, D.; Liang, X. Synthesis and antifungal activity of seven oleanolic acid glycosides. *Molecules* **2011**, *16*, 1113-1128.
[39] Matin, M.M.; Bhuiyan, M.M.H.; Debnath, D.C.; Manchur, M.A. Synthesis and comparative antimicrobial studies of some acylated D-glucofuranose and D-glucopyranose derivatives. *Int. J. Biosci*.**2013**, *3*, 279-287.
[40] Nizamov, I.S.N.; Yevgeniy, N.; Nizamov, Ilnar D.; Belov, T.G.; Voloshina, A.D.; Batyeva, E.S.; Cherkasov, R.A. α-d-Glucofuranose and α-d-allofuranose diacetonides and silyl ether of α-D-glucofuranose diacetonide in dithiophosphorylation reactions. *Heteroat. Chem.* **2016**, *27*, 345-352.
[41] Islam, N.; Islam, M.D.; Rahman, M.R.; and Matin, M.M. Octyl 6-O-hexanoyl-β-D-glucopyranosides: Synthesis, PASS, antibacterial, in silico ADMET, and DFT studies. *Curr. Chem. Lett.* **2021**,*10*(*4*), 413-426.
[42] Matin, M.M.; Bhattacharjee, S.C.; Chakraborty, P.;Alam, M.S. Synthesis, PASS predication, in vitro antimicrobial evaluation and pharmacokinetic study of novel n-octyl glucopyranoside esters. *Carbohydr. Res.* **2019**, *485*, 107812.
[43] Rao, V.U.S.; Arakeri, G.; Madikeri, G.; Shah, A.; Oeppen, R.S.; Brennan, P.A. Post-COVID Mucormycosis in India: A formidable challenge. *Br. J. Oral Maxillofac. Surg*. **2021**, *59*, 1095-1098.
[44] Kumer, A.; S. Paul, S.; Sarker, M.N.; Islam, M.J. The prediction of thermo physical, vibrational spectroscopy, chemical reactivity, biological properties of morpholinium borate, phosphate, chloride and bromide ionic liquid: A DFT study. *Int. J. New Chem.* **2019**, *6*, 236-253.
[45] Kumer, A.; Sarker, M.N.; Paul, S.; The theoretical investigation of HOMO, LUMO, thermophysical properties and QSAR study of some aromatic carboxylic acids using Hyper Chem programming. *Int. J. Chem.* **2019**, *3*, 26-37.
[46] Islam, M.J.;Sarker, M.N.; Kumer, A.; Paul, S. The evaluation and comparison of thermo-physical, chemical and biological properties of palladium(II) complexes on binuclear amine ligands with different anions by DFT study. *Int. J. Adv. Biol.* **2019**, *7*, 318-337.
[47] Islam, M.J.;Kumer, A.; Sarker,M.N.; Paul, S.; Zannat, A. The prediction and theoretical study for chemical reactivity, thermophysical and biological activity of morpholinium nitrate and nitrite ionic liquid crystals: A DFT study. *Adv. J. Chem. Sect. A* **2019**,*2*, 316-326.
[48] Islam, M.J.; Kumer, A.; Paul, S.; Sarker, M.N. The activity of alkyl groups in morpholinium cation on chemical reactivity, and biological properties of morpholinium tetrafluroborate ionic liquid using the DFT method. *Chem. Methodol.* **2020**, *4*, 130-142.
[49] Kadir, F.A.; Kassim, N.M.; Abdulla, M.A.;Yehye, W.A. PASS-predicted *Vitex negundo* activity: antioxidant and antiproliferative properties on human hepatoma cells-an in vitro study. *BMC Complement Altern. Med*. **2013**, *13*, 1-13.

[50] Ramos, J. Introducción a materials Studio en la investigación química y ciencias de los materiales. **2020**, (http://hdl.handle.net/10261/96382).

[51] Delley, B. Time dependent density functional theory with DMol3. *J. Phys. Conf. Condensed Matter* **2010**, *22*, 384208.

[52] Zhou, X.; Gao, Y.; Wang, W.; Yang, X.; Yang, X.; Liu, F.; Tang, Y.; Lam, S.M.; Shui, G.; Yu, L. Architecture of the mycobacterial succinate dehydrogenase with a membrane-embedded Rieske FeS cluster. *PNAS* **2021**, *118*, e2022308118

[53] Cánovas-Márquez, J. T.; Falk, S.; Nicolás, F.E.; Padmanabhan, S.; Zapata-Pérez, R.; Sánchez-Ferrer, Á.; Navarro, E.; Garre, V. A ribonuclease III involved in virulence of Mucorales fungi has evolved to cut exclusively single-stranded RNA. *Nucleic Acids Res.* **2021**, *49*, 5294-5307.

[54] Qin, Z.; Yan, Q.; Lei, J.; Yang, S.; Jiang, Z.; Wu, S. The first crystal structure of a glycoside hydrolase family 17 β-1, 3-glucanosyltransferase displays a unique catalytic cleft. *Acta Cryst. Sect. D: Biol. Crystallogr.* **2015**, *71*, 1714-1724.

[55] Michalska, K.; Evdokimova, E.; Semper, C.; Di Leo, R.; Stogios, P.J.; Savchenko, A.; Joachimiak, A. Crystal structure of 3-deoxy-D-arabinoheptulosonate-7-phosphate synthase/phospho-2-dehydro-3-deoxyheptonate aldolase (Aro3) from *Candida auris*. *Protein Data Bank*, **2019**.

[56] Fushinobu, S.; Ito, K.; Konno, M.; Wakagi, T.; Matsuzawa, H. Crystallographic and mutational analyses of an extremely acidophilic and acid-stable xylanase: biased distribution of acidic residues and importance of Asp37 for catalysis at low pH. *Protein Engineering* **1998**, *11*, 1121-1128.

[57] Tonthat, N.K.; Juvvadi, P.R.; Zhang, H.; Lee, S.C.; Venters, R.; Spicer, L.; Steinbach, W.J.; Heitman, J.;Schumacher, M.A. Structures of pathogenic fungal FKBP12s reveal possible self-catalysis function. *mBio*, **2016**, *7*, e00492-00416.

[58] DeLano, W.L. The PyMOL user's manual. **2002**. http://www.pymol.org

[59] Dallakyan, S.;Olson, A.J. Small-molecule library screening by docking with PyRx. In *Chemical Biology*, **2015**, pp 243-250, Springer.

[60] Inc, A.S. Discovery Studio Modeling Environment, Release 4.0, Accelrys Software Inc San Diego.**2017**.

[61] Feixiong Cheng, F.; Li, W.; Zhou, Y.; Jie Shen, J.; Wu, Z.; Liu, G.; Lee, P.W.; Tang, Y. admetSAR: a comprehensive source and free tool for assessment of chemical ADMET properties. *J. Chem. Inf. Model*. **2012**, *52*, 3099-3105.

[62] Matin, M.M.; Islam, N.; Siddika, A.; Bhattacharjee, S.C. Regioselective synthesis of some rhamnopyranoside esters for PASS predication, and ADMET studies. *J. Turk. Chem. Soc. Sect. A: Chem.***2021**, *8*(*1*), 363-374.

[63] Yang, H.; Lou, C.; Sun, L.; Li, J.; Cai, Y.; Wang, Z.; Li, W.; Liu, G.; Tang, Y. admetSAR 2.0: web-service for prediction and optimization of chemical ADMET properties. *Bioinformatics* **2019**, *35*, 1067-1069.

[64] De Oliveira, D.B.; Gaudio, A.C. BuildQSAR: a new computer program for QSAR analysis, quantitative structure-activity relationships. *Mol. Inform.* **2001**, *19*, 599-601.

[65] Lipinski, C.A.; Lombardo, F.; Dominy, B.W.; Feeney, P.J. Experimental and computational approaches to estimate solubility and permeability in drug discovery and development settings. *Adv. Drug Delivery Rev.***1997**, *23*, 3-25.

[66] Parr, R.G.; Robert, A.D.; Levy, M.; Palke, W.E. Electronegativity: the density functional viewpoint. *J. Chem. Phys.***1978**, *68*, 3801-3807.

[67] Parr, R.G.; Szentpály, L.V.; Liu, S. Electrophilicity index. *J. Am. Chem. Soc.***121**, *1999*, 1922-1924.

[68] Hoque, M.M.H.; Sajib, M.; Kumer, A.;Wahab, K.M. Synthesis of 5, 6-diaroylisoindoline-1, 3-dione and computational approaches for investigation on structural and mechanistic insights by DFT. *Mol Simul.***2020**, *36*, 1298-1307.

[69] Kawsar, S.; Kumer, A. Computational investigation of methyl α-D-glucopyranoside derivatives as inhibitor against bacteria, fungi and COVID-19 (SARS-2). *J. Chil. Chem. Soc*. **2021**, *66*, 5206-5214.

[70] Kumer, A.; Sarker, M.N.; Paul, S.; Zannat, A. The theoretical prediction of thermophysical properties, HOMO, LUMO, QSAR and biological indices of cannabinoids (CBD) and tetrahhdrocannabinol (THC) by computational chemistry. *Adv. J. Chem. Sect. A***2019**, *2*, 190-202.

[71] Kumer, A.; Sarker, M.N.; Paul, S. The thermo physical, HOMO, LUMO, Vibrational spectroscopy and QSAR study of morphonium formate and acetate ionic liquid salts using computational method. *Turk. Comput. Theor. Chem.* **2019**, *3*, 59-68.

[72] Kumer, A.; Sarkar, M.N.; Pual, S. The simulating study of HOMO, LUMO, thermo physical and quantitative structure of activity relationship (QSAR) of some anticancer active ionic liquids, *Eurasian J. Environ. Res.* **2019**, *3*, 1-10.

[73] Hanee, U.; Rahman, M.R.; Matin, M.M. Synthesis, PASS, in silico ADMET, and thermodynamic studies of some galactopyranoside esters. *Phys. Chem. Res.* **2021**, *9*(*4*), 591-603.

[74] Cosconati, S.; Forli, S.; Perryman, A.L.; Harris, R.; Goodsell, D.S.; Olson, A.J. Virtual screening with AutoDock: theory and practice. *Expert Opin. Drug Discov.* **2010**, *5*, 597-607.

[75] Kumer, A.; Khan, M.W. The effect of alkyl chain and electronegative atoms in anion on biological activity of anilinium carboxylate bioactive ionic liquids and computational approaches by DFT functional and molecular docking. *Heliyon* **2021**, e07509.

[76] Kumer, A.; Khan, M.W. Synthesis, characterization, antimicrobial activity and computational explorations of ortho toludinium carboxylate ionic liquids. *J. Mol. Struct.***2021**, 131087.

[77] Nath, A.; Kumer, A.; Zaben, F.; Khan, M. W. Investigating the binding affinity, molecular dynamics, and ADMET properties of 2, 3-dihydrobenzofuran derivatives as an inhibitor of fungi, bacteria, and virus protein, *Beni-Seuf. Univ. J. Appl*. **2021**, *10*, 1-13.

[78] Nath, A.; Kumer, A.; Khan, M.W. Synthesis, computational and molecular docking study of some 2, 3-dihydrobenzofuran and its derivatives .*J. Mol. Struct* . **2020**, *1224*, 129-225.

[79] Talarico, C.; Gervasoni, S.; Manelfi, C.; Pedretti, A.; Vistoli, G.;Beccari, A.R. Combining molecular dynamics and docking simulations to develop targeted protocols for performing optimized virtual screening campaigns on the HTRPM8 channel. *Int. J. Mol. Sci.* **2020**,*21*, 2265.